Complexes of Iron(II) with Silylated Pentalene Ligands; Building Blocks for Homo- and Heterobimetallics

Alexander F. R. Kilpatrick,[‡] David R. Johnston,[‡] Jennifer C. Green,[§] Nikolaos Tsoureas,[‡] Martyn P. Coles,[‡] and F. Geoffrey N. Cloke.*[‡$]

[‡] Department of Chemistry, School of Life Sciences, University of Sussex, Brighton, BN1 9QJ, UK

[§] Department of Chemistry, University of Oxford, Inorganic Chemistry Laboratory, South Parks Road, Oxford, OX1 3QR, UK

[$]*Dedicated to Malcolm Green on the occasion of his 80th birthday, with deepest thanks for his inspiration, support and friendship for more than 40 years*

ABSTRACT

A range of iron(II) complexes incorporating the silylated pentalene ligands ($Pn^{\ddagger}H$ = 1,4-$\{Si^iPr_3\}_2C_8H_5$ and $Pn^{\ddagger}$ = 1,4-$\{Si^iPr_3\}_2C_8H_4$) have been investigated as model molecules/building blocks for metallocene-based polymers. Six complexes have been synthesised and extensively characterised by a range of techniques, including by cyclic voltammetry and X-ray diffraction studies. Amongst these compounds are the homobimetallic $[Cp^*Fe]_2(\mu\text{-}Pn^{\dagger})$ which is a fused analogue of biferrocene, and the 3*d*/4*s* heterobimetallic $[Cp^*Fe(\eta^5\text{-}Pn^{\dagger})][K]$ which forms an organometallic polymer in the solid state. DFT calculations on model mono-Fe(η^5-Pn) compounds reveal the charge densities on the uncoordinated carbon atoms of the pentalene ligand, and hence the potential for incorporating these units into heteronuclear bimetallic complexes is assessed.

KEYWORDS

iron; organometallic polymer; pentalene; homobimetallic; heterobimetallic

INTRODUCTION

Molecules containing more than one metal centre can exhibit profoundly different physical properties and reactivity compared to monometallic complexes, particularly where there is a strong interaction between the metal centres.[1-4] The synthesis of polymers which contain metallocene units in close proximity is highly desirable as it should allow extended metal–metal interactions throughout the chain,

which may result in novel electronic, magnetic or other physical properties.[5] The aromatic ligand pentalene (Pn, C_8H_6) has shown ability to delocalise electron density between metal centres in anti-bimetallic transition metal compounds, and promote coupling effects through the planar π-system of the bridging Pn ligand.[6] Metal-metal interactions have been studied extensively by Manriquez *et al.* for the capped triple-decker complexes $[Cp^*M(\mu\text{-}\eta^5\text{:}\eta^5\text{-Pn})MCp^*]^{n+}$ with transition metals (Fig. 1a, M = Fe, Co, Ni, Ru) using a variety of physical techniques.[7-10] Cyclic voltammetry (CV) revealed that these compounds undergo two successive one-electron transfers, with large potential separations between successive oxidations ($\Delta E_{½}$, decreasing in the order Fe > Co > Ni > Ru). Oxidation to the cationic forms (n = +1 and +2) was achieved for each complex, of which the mixed-valence (MV) forms (n = +1) show IVCT bands in the NIR spectrum that are not observed in the neutral or di-cationic forms. ^{57}Fe Mössbauer spectroscopy (timescale ≈ 10^{-7} s) studies of the cationic $[Cp^*Fe(\mu\text{-}\eta^5\text{:}\eta^5\text{-Pn})FeCp^*]^+$ species found the iron environment to be fully averaged down to 1.5 K, indicative of a strong electronic interaction between the metal centres and extensive delocalisation in the MV state.

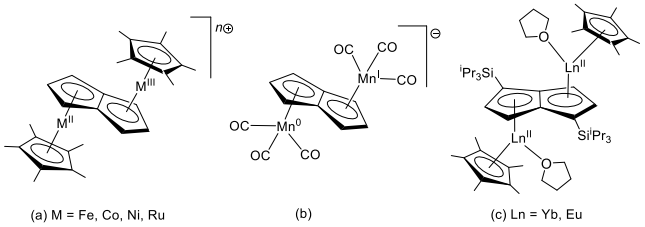

Fig. 1. Examples of anti-bimetallic complexes studied for metal-metal interactions.

O'Hare *et al.* reported anti-bimetallic complexes of group 7 metal carbonyls, $[M(CO)_3]_2(\mu\text{:}\eta^5,\eta^5\text{-Pn})$ (M = Mn and Re) and showed that the manganese species may be reduced by electrochemical or chemical methods to yield both the dianion as a dilithium salt, and the mono-anion stabilised by a $[FeCp(C_6Me_6)]^+$ counterion (Fig. 1b). The latter is formally a Mn(I)/Mn(0) mixed-valence complex with two equivalent metal centres on the EPR spectroscopic timescale, consistent with a Robin-Day class III system.[11] This MV anion remains one of the most delocalised organometallic systems reported to date. In our laboratory we have extended these anti-bimetallic complexes to the f-block metals using silylated pentalene ligands, in complexes of the type $[Cp^*Ln(THF)]_2(\mu\text{:}\eta^5,\eta^5\text{-Pn}^\dagger)$ ($Pn^\dagger$ = 1,4-$\{Si^iPr_3\}_2C_8H_4$; Ln = Eu and Yb, Fig. 1c),[12] which are of interest as molecular models for

lanthanide-based polymers.[13,14]

Despite the number of pentalene-bridged homobimetallic compounds of the general formula $L_nM(\mu\text{-}\eta^5\text{:}\eta^5\text{-Pn})M'L_n'$ (M = M') that have been synthesised, comparatively few heterobimetallic (M ≠ M') examples are known. The main synthetic challenge is selective coordination of two different metal centres to the pentalene bridge to give a mixed-metal complex, whilst preventing formation of homobimetallic species. Strategies for the rational synthesis of such materials were pioneered by Manriquez *et al.* starting with dihydropentalene *via* successive deprotonation and incorporation of the appropriate metal 'half-sandwich' synthon (Scheme 1),[7] in the so-called 'building block' route.

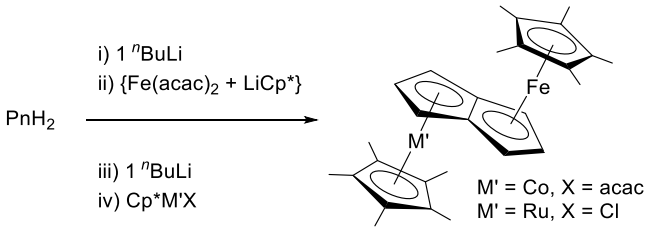

Scheme 1. 'Building block' synthetic route to heterobimetallics.[7]

In a modification of the 'building block' synthetic approach, $Fe(\eta^5\text{-PnH})_2$ was lithiated *in situ* and used to incorporate a Cp*Co unit into the chain, forming $Cp^*Co(\mu\text{-}\eta^5\text{:}\eta^5\text{-Pn})Fe(\eta^5\text{-PnH})$ (Fig. 2a), classified as an *asymmetric* anti-bimetallic due to the different ligand environments of the two metals ($L_n \neq L_n'$).[8] Interestingly the introduction of asymmetry in the ligand environment in $[Cp^*Co(\mu\text{-}\eta^5\text{:}\eta^5\text{-Pn})Fe(\eta^5\text{-PnH})]^+$ leads to Class I "valence trapped" behavior based on the electrochemical (CV) and spectroscopic (NIR, Mössbauer) evidence,[9] whereas the symmetric congener $[Cp^*Co(\mu\text{-}\eta^5\text{:}\eta^5\text{-Pn})FeCp^*]^+$ is Class II. It was suggested that ligand asymmetry in general introduces a barrier for electron transfer and as a result decreases the extent of electronic interaction. This has a larger impact for heteronuclear complexes which already have an built-in barrier for electron transfer from the different electronic nature of the metal centres, and the subtle effect of changing the terminal ligand in this case can cause some loss of electronic communication.

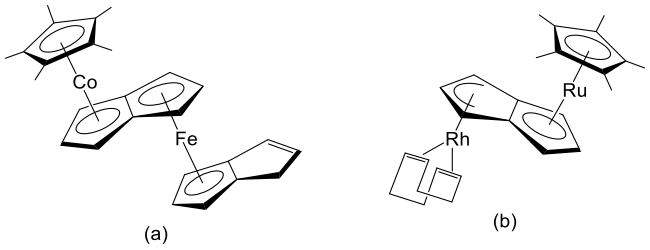

Fig. 2. Examples of hetero-bimetallics with asymmetric ligand environments.

The synthesis of oligomeric or polymeric materials consisting of alternating metal atoms and fused-ring ligands is expected to offer a range of interesting delocalised properties.[1] Strategies for the rational synthesis of such materials were pioneered by Manriquez *et al.* who extended work on bimetallic pentalene systems described above to incorporate further organometallic fragments into the chain.[8] The fully capped trimetallic complex $(Cp^*Fe)_2[Pn_2Fe]$ was synthesised from $Fe(\eta^5\text{-}PnH)_2$ by lithiation with ^{n}BuLi followed by addition of FeCp*(acac) in two successive iterations (Scheme 2a). A potentially iterative process to higher chain oligomers was presented in the synthesis of a novel quadruple decker iron-pentalene complex from reaction of [Li][PnFe(η^5-PnH)] with 0.5 equivalents of $Fe(acac)_2$ in THF (Scheme 2b). The quadruple-decker complex $(\{\eta^5\text{-}PnH\}Fe)_2[Pn_2Fe]$ was characterised by mass spectrometry and IR spectroscopy, however NMR and structural characterisation by single crystal XRD were hampered by its low solubility in hydrocarbon solvents (400 mg L^{-1} of boiling toluene), and this has prevented synthesis of higher chain oligomers.

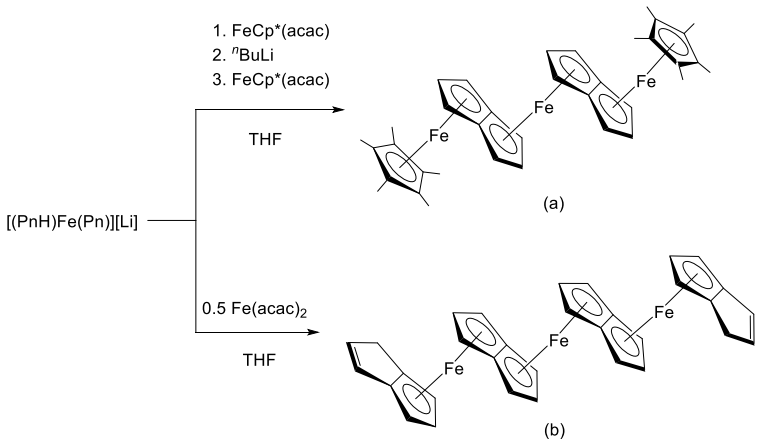

Scheme 2. Synthetic routes to trimetallic pentalene complexes.[8]

Subsequent studies by other research groups employing alkylated (Pn^R = {1-R}C_8H_5) or silylated (Pn' = 1,4-{$SiMe_3$}$_2C_8H_4$) pentalene ligands have successfully introduced a greater degree of solubility in hydrocarbon solvents to the resulting iron(II) complexes.[15,16] However due to the lack of symmetry in these ligands, a mixture of isomeric multi-decker species were isolated as oils which could not be purified, precluding full characterisation. The formation of multiple isomers also prevented unambiguous assignment of the electrochemical data obtained, and their potential as delocalised organometallic polymers could not be fully determined.

Herein, we describe the synthesis and characterisation of well-defined Fe(II) complexes by virtue of the high steric demands of the 1,4-triisopropylsilyl substituted hydropentalene ($Pn^{\dagger}H$) ligand. The utility of these complexes towards the synthesis oligomeric and heteronuclear organometallic complexes is explored using the 'building block' synthetic approach, in which deprotonation of the uncoordinated ring of a bound $Pn^{\dagger}H$ ligand provides an opportunity for coordination of the resultant anion to other metal units.

RESULTS AND DISCUSSION

Iron Bis(pentalene) Complexes

*Synthesis and characterisation of Fe(η^5-$Pn^{\dagger}H$)$_2$ (**1**)*

The homoleptic iron(II) complex Fe(η^5-$Pn^{\dagger}H$)$_2$ (**1**) was targeted as a convenient entry point for these synthetic studies. **1** was prepared by reaction of the hydropentalenyl mono-potassium salt [K]$Pn^{\dagger}H$ with $FeCl_2(THF)_{1.1}$ in THF at -78 °C which gave a red suspension upon warming to room temperature. After pentane work-up a crude red solid was isolated which was recrystallised from Et_2O at -50 °C to afford **1** in 65% yield (Scheme 3).

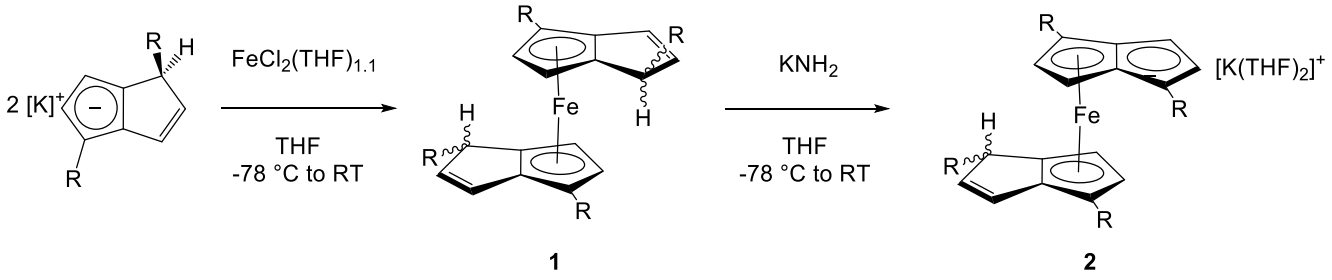

Scheme 3. Synthesis of **1** and **2**. R = Si^iPr_3.

The $Pn^{\dagger}H$ ligand is facially enantiotopic, hence its sandwich complexes would be expected to exist, in principle, as different diastereomers. In an idealised conformation with the frameworks of the carbocyclic rings eclipsed, there are two possible arrangements of the 1,4-$Si^{i}Pr_3$ substituents on each ligand; eclipsed and staggered. With eclipsed $Si^{i}Pr_3$ groups on each ligand three diastereomers are possible (Scheme 4), two with the $Si^{i}Pr_3$ groups on the sp^3 carbon of the uncoordinated ring mutually *exo* and *endo* (*S,R* and *R,S*) and one diastereomer that exists as a pair of enantiomers (*R,R* and *S,S*). A 180° rotation about one Fe–centroid bond would relieve the relative strain energy due to the bulky $Si^{i}Pr_3$ groups.

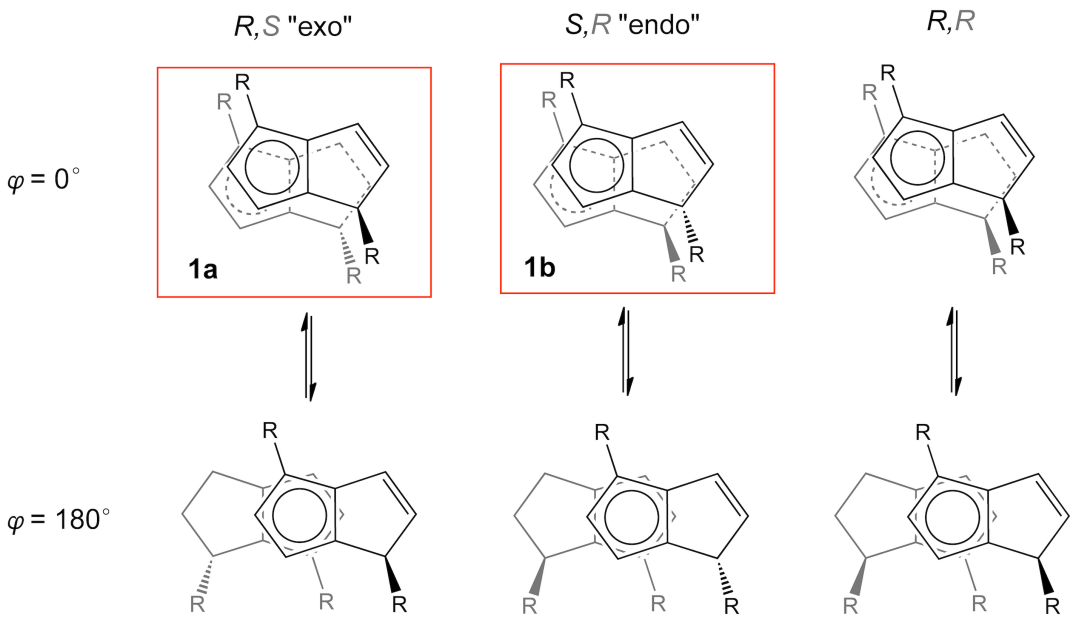

Scheme 4. Possible isomers of **1** with eclipsed 1,4-R (= $Si^{i}Pr_3$) substituents. The *S,S* stereoisomer has been omitted for clarity.

A further three diastereomers are possible with $Si^{i}Pr_3$ groups staggered (in a conformation with the two pentalene frameworks eclipsed); again one *exo*, one *endo* and one chiral (Scheme 5). A 180° rotation about one Fe–centroid bond this time introduces symmetry to the *R,R* and *S,S* diastereomers.

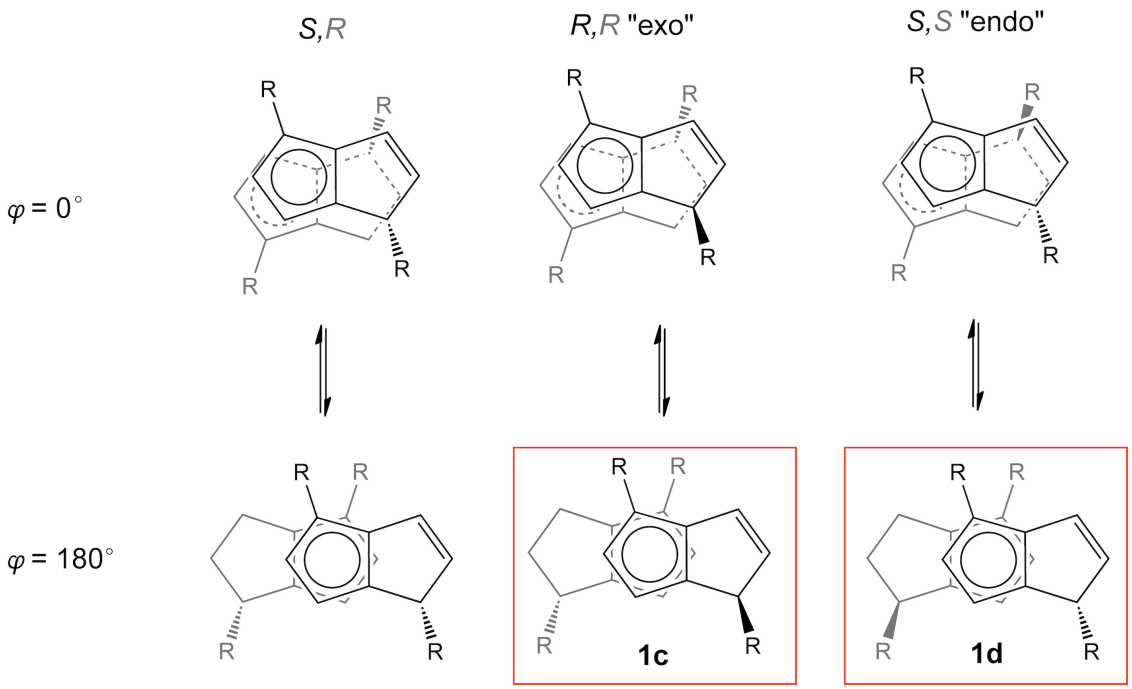

Scheme 5. Possible isomers of **1** with staggered 1,4-R (= Si^iPr_3) substituents.

The *R,S* stereoisomer has been omitted for clarity.

Given that the room temperature ^{1}H NMR spectrum of **1** shows five Pn†H ring signals per isomer, the two ligands must be related by symmetry over the timescale of the experiment, which implies **1a-d** as possible structures (outlined in red in Schemes 4 and 5). It is proposed that the extra strain of the Si^iPr_3 groups pointing in towards the rest of the molecule in an *endo* conformation would make these isomers less favourable energetically. Therefore **1a** and **1c** are proposed as the two isomers formed. The stereochemistry of the crystallographically characterised molecule (Fig. 3) corresponds to that of diastereomer **1a**, adopting a conformation in the solid state with a dihedral angle (φ, defined by the angle between the mean planes of the Fe atom and the wing-tip C atoms of the two Pn†H ligands, see Fig. 4) of 113.88(7)° that lies between the two idealised conformations depicted in Scheme 4. Assuming in solution the energy barrier to rotation about the metal-centroid bonds is small in comparison with k_BT, the two Pn†H rings within each isomer are chemically equivalent on the NMR timescale.

*Synthesis and characterisation of (η^5-Pn†H)Fe[η^5-Pn†(η^5-K{THF}$_2$)] (**2**)*

Facile mono and double deprotonation of Katz's Fe(η^5-PnH)$_2$ complex was achieved using *n*- and *t*-butyllithium,[17] showing that the allylic proton on the uncoordinated ring of the hydropentalenyl

ligand is relatively acidic. The ligand fragment produced, effectively a pentalenyl dianion, would have stability as a fully delocalised 10π electron aromatic system. It was proposed the trialkylsilyl-substituted hydropentalenyl ligands in **1** may be relatively more acidic than their unsubstituted equivalents in Fe(η^5-PnH)$_2$, given that the allylic proton is α- to silicon.[18,19] However, **1** proved to be surprisingly unreactive towards many strong bases, and no reaction was observed with *n*- or *t*-BuLi/TMEDA, KH, K(N{SiMe$_3$}$_2$), Bu$_2$Mg, or Ca(N{SiMe$_3$}$_2$)$_2$. Reaction of **1** with two equivalents of potassium amide in THF at -78 °C, resulted in a red-green colour upon warming to room temperature. Work-up and recrystallisation from pentane at -50 °C afforded dark red crystals which were identified by XRD analysis as the mono-deprotonated species, **2** (Scheme 3).

The molecular structure of **2** is shown in Fig. 3 and key metrical parameters for **1** and **2** are collated in Table 1. These sandwich structures have very similar geometries around the Fe centre, with metal-centroid distances and near linear centroid–metal–centroid angles which are consistent with ferrocene and its pentalene analogues that have been previously determined by X-ray diffraction studies.[20-24] Removal of an allylic proton from **1** to form **2** results in a formal negative charge on the five membered ring of the coordinated pentalene ligand, to which potassium coordinates in an η^5- mode. The K–C$_{ring}$ bond lengths for **2** lie in the range 2.943(4) - 3.046(4) Å, which are comparable with potassium cyclopentadienyl derivatives such as [K-C$_5$H$_4${SiMe$_3$}]$_n$ (2.988(8) - 3.074(10) Å).[25]

Key structural differences are found in the carbocyclic ligands when comparing compounds bearing a Pn†H ligand with one C$_5$-ring that is not coordinated to a metal, such as **1**, with bimetallic complexes bearing a dianionic Pn† ligand, such as **2**. In particular the C6–C7 bond for **1** (1.339(3) Å) is significantly shorter than the other C–C distances in the pentalene skeleton (1.421(3) - 1.517(3) Å). This is consistent with a localised double bond, and similar values are found in previously reported hydropentalenyl compounds Fe(η^5-PnH)$_2$,[20] [Re(CO)$_3$](η^5-PnH),[26] and (η^8-Pn†)Sm(η^5-Pn†H),[27] ($d_{C=C}$ = 1.329(8), 1.377(9) and 1.354(7) Å respectively).

The C2–C1–Si1 bond angles for **1** and **2** (126.85(18)° and 125.0(2)° respectively) are consistent with a near planar C1 in the η^5-coordinated ring of both Pn†H and Pn† ligands. This contrasts with the C7–C8–Si2 angles (115.08(17)° and 125.3(3)° respectively), which are significantly smaller for **1** illustrating the near tetrahedral geometry of the allylic C8 in the uncoordinated ring of these complex. The allylic protons H8 and H27 in **1** are arranged *endo* to the Fe centre and are sterically shielded by the *exo* Si^{i}Pr$_3$ groups, which is a possible reason for the difficulty of deprotonation at these positions with strong bases such as ^{t}BuLi. If a neutral electron counting scheme (CBC) is employed,[28] both

Pn† and Pn†H ligands serve as 5 electron donors (L_2X) to each metal centre in η^5-mode, but in the Pn†H case the π-electron density is only delocalised around one half of the pentalene skeleton.[17,29] This is reflected in shorter Fe–Ct1 distances and smaller Δ values for **1** compared with **2**.

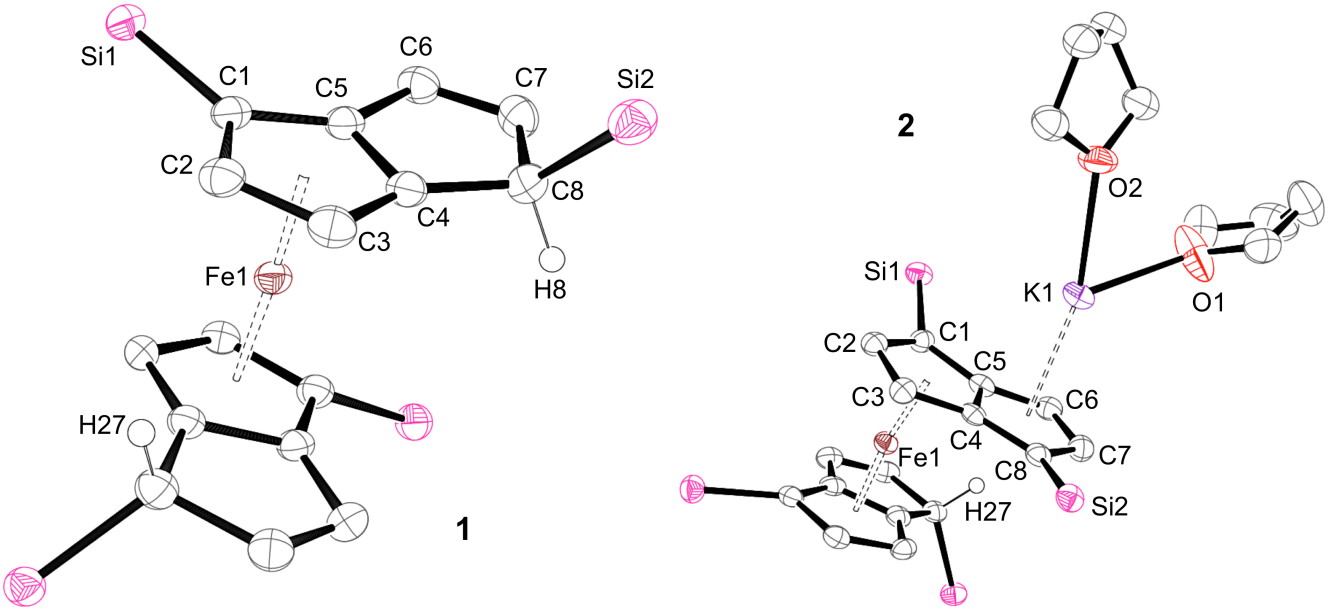

Fig. 3. Displacement ellipsoid plots (50% probability) of **1** and **2**.
Hydrogen atoms (except allylic H's) and ^{i}Pr groups omitted for clarity.

Table 1. Selected distances (Å), angles (°) and parameters (defined in Fig. 4) for **1** and **2**. Ct1 and Ct3 correspond to the η^5-centroids of the Pn1 and Pn2 rings respectively.

Parameter	**1**	**2**
Fe–C1	2.086(2)	2.085(3)
Fe–C2	2.022(2)	2.024(4)
Fe–C3	2.051(2)	2.065(5)
Fe–C4	2.098(2)	2.173(4)
Fe–C5	2.094(2)	2.120(3)
φ	113.9	95.7
$\Delta_{\text{Fe-Ct1}}$	0.043	0.089
Fe–Ct1	1.6731(11)	1.6936(5)

Fe–Ct3	1.6719(10)	1.6756(5)
Ct1–Fe–Ct3	173.48(5)	170.83(8)
C1–C2	1.451(3)	1.454(5)
C2–C3	1.429(3)	1.429(5)
C6–C7	1.339(3)	1.384(6)
C7–C8	1.517(3)	1.423(5)
av. C–C_{ring}	1.444(3)	1.436(5)
C2–C1–Si1	126.85(18)	125.0(2)
C7–C8–Si2	115.08(17)	125.3(3)
Fe···K	-	4.773

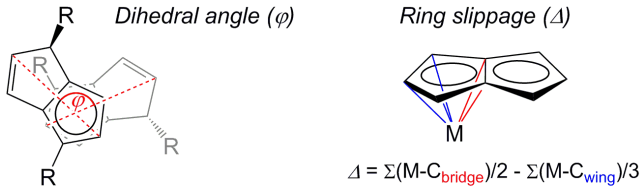

Fig. 4. Definition of the geometric parameters φ and Δ.

Complex **2** was found to be extremely air and moisture sensitive, and satisfactory elemental analysis could not be obtained despite repeated attempts and attributed to the lability of the coordinated THF. Furthermore, the ^{1}H NMR spectrum in THF-d_8 was complex and could not be assigned unambiguously. Subsequent attempts to doubly deprotonate **1** using an excess of KNH_2 and 18-crown-6 were unsuccessful, yielding complex **2** exclusively. Hence, attempts were made to incorporate further organometallic fragments into **2**, by reaction with divalent metal salts ($FeCl_2(THF)_{1.1}$, $Fe(acac)_2$ and YbI_2) and mono-Cp* complexes (Cp*Fe(acac), Cp*FeCl(TMEDA)). However, in all cases the products isolated after work-up were identified by EI-MS and NMR spectroscopy as $Fe(\eta^5\text{-}Pn^{\dagger}H)_2$, present as mixture of three diastereomers. Clearly the decomposition of **2** to **1** in these reactions involves protonation of a bound $Pn^{\dagger}$ ligand. The fact that **1** is produced as a mixture of diastereomers suggests protonation of the planar pentalene ring occurs in a stereochemically undefined process, and therefore likely to arise from an intermolecular decomposition reaction or by solvent activation.

Mixed-Sandwich Iron Complexes

*Synthesis and characterisation of Cp*Fe(η^5-Pn†H) (**3**)*

An alternative route to heterobimetallics was explored *via* mixed-sandwich complexes, with Pn†H and Cp* ligands, which possess higher symmetry allowing for more straightforward interpretation of NMR spectra and potentially avoid the formation of isomers complicating the situation. Synthesis of **3** was achieved by reaction of [K]Pn†H with Cp*FeCl(TMEDA) in THF, which following work-up, was isolated as orange crystals in 81% yield (Scheme 6). Mass spectrometry and elemental analysis confirmed the identity and purity of the product. ^{1}H, ^{13}C{^{1}H} and ^{29}Si{^{1}H} NMR spectroscopy showed the existence of a single species and the spectra correspond to the proposed structure. The latter was ultimately confirmed by a single crystal XRD study (Fig. 5).

Synthesis and characterisation of [FeCp(μ-η^5:η^5-Pn†)][K] (**4**)*

With a view to extending the metal-pentalene chain of **3**, the 'building block' synthetic approach was again pursued, in which deprotonation of the uncoordinated ring of a bound Pn†H ligand would provide an opportunity for coordination of the resultant anion to other metal units. However, as found with the homoleptic analogue **1**, complex **3** was unreactive with many strong bases, including ^{t}BuLi, MeLi, $NaNH_2$, MeK and KH. Given that Manriquez *et al.* reported that deprotonation of the unsubstituted complex Cp*Fe(η^5-PnH) is facile with ^{n}BuLi, it is clear that the bulky *exo* Si^{i}Pr$_3$ group hinders removal of the allylic proton in **3** (H8 in Fig. 3).

Reaction of **3** with an excess of KNH_2 in THF-d_8 resulted in a colour change from orange to dark red over 4 days. ^{1}H NMR spectroscopy of the red solution after filtration revealed complete disappearance of the five pentalene ring signals for **3** and the appearance of a new set of peaks, including four doublets in equal ratio which were assigned to an aromatic pentalenyl ligand. ^{29}Si{^{1}H} NMR showed two peaks indicating an asymmetric Pn† ring and the formulation of a deprotonated species [Cp*Fe(μ-η^5:η^5-Pn†)][K] (**4**) was proposed. ^{1}H, ^{13}C and ^{29}Si NMR assignments were corroborated through the use of two dimensional ^{1}H-^{1}H, ^{13}C-^{1}H and ^{29}Si-^{1}H correlation experiments. Single crystals of **4** suitable for XRD studies were grown from Et_2O and the molecular structure is shown in Fig. 5.

The anion-cation pair **4** is extremely sensitive to air and moisture, readily decomposing to afford, *inter alia*, complex **3** unless the most stringent precautions are taken with all glassware and solvents. Furthermore, solutions of **4** in THF are unstable upon solvent removal *in vacuo*; an NMR tube containing a spectroscopically pure sample of **4** in THF-d_8 was carefully exposed to dynamic vacuum,

taken to dryness, and then redissolved in C_6D_6. The ^{1}H NMR spectrum of the resulting solution showed the presence of **3** with the appearance of five new ring H signals, corresponding to a previously unidentified decomposition product, **5**, in *ca.* 25% conversion. Compound **5** was separated from the reaction mixture by toluene extraction and recrystallisation from Et_2O. Single crystal XRD analysis identified these green crystals as Cp*Fe(η^5-C_8H_5{Si^{i}Pr$_3$-1,4}$_2$) (**5**), the double bond isomer of **3** (Fig. 5). The ^{1}H NMR spectrum of **5** showed two allylic H signals at 2.93 and 2.67 ppm, with a geminal coupling ($^2J_{HH}$ = 21.5 Hz) corroborating the migration of the C=C double bond. Complex **5** was further characterised by ^{13}C{^{1}H} and ^{29}Si{^{1}H} NMR spectroscopy, mass spectrometry and elemental analysis. The deprotonation of mixed-sandwich iron complex **3** to form **4**, and the subsequent decomposition pathway of the latter are summarised in Scheme 6.

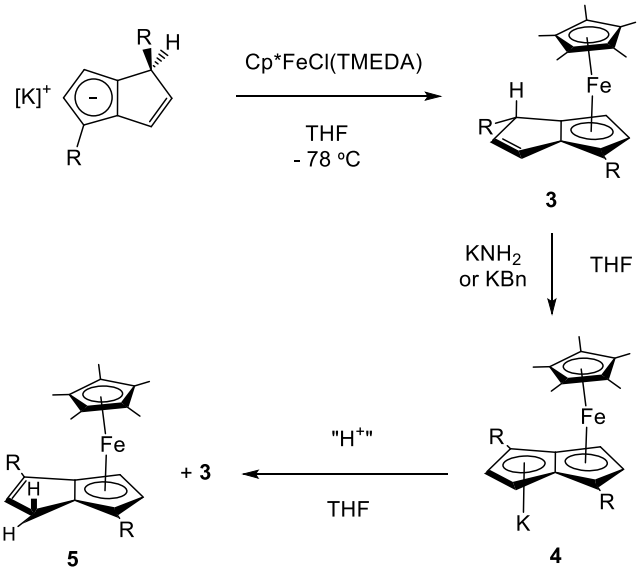

Scheme 6. Synthesis and reactivity of **3** and **4** (R= Si^{i}Pr$_3$).

*X-ray crystallographic studies of **3**, **4** and **5***

As found for **1** and **2**, there are variations in ligand bond lengths and angles of the complexes with Pn†H ligands (**3** and **5**) compared with Pn† (**4**). Comparing **5** and **3**, which can be considered as isomers of Cp*Fe(η^5-Pn†H), reveals a decrease in distance C7–C8 of 0.091 Å and an elongation along C6–C7 of 0.059 Å, which is consistent with the migration of the double bond. Inspection of the metal-centroid distances shows that the mono-metallated Pn†H ligand in **3** and **5** allows for closer coordination of the Fe centre compared with the di-metallated Pn† ligand in **4**. This situation is also observed between the two ligands in **2** and other bimetallic iron complexes, [Cp*M](μ-η^5:η^5-Pn)[Fe(PnH)] where M = Fe or Co.[23],[22]

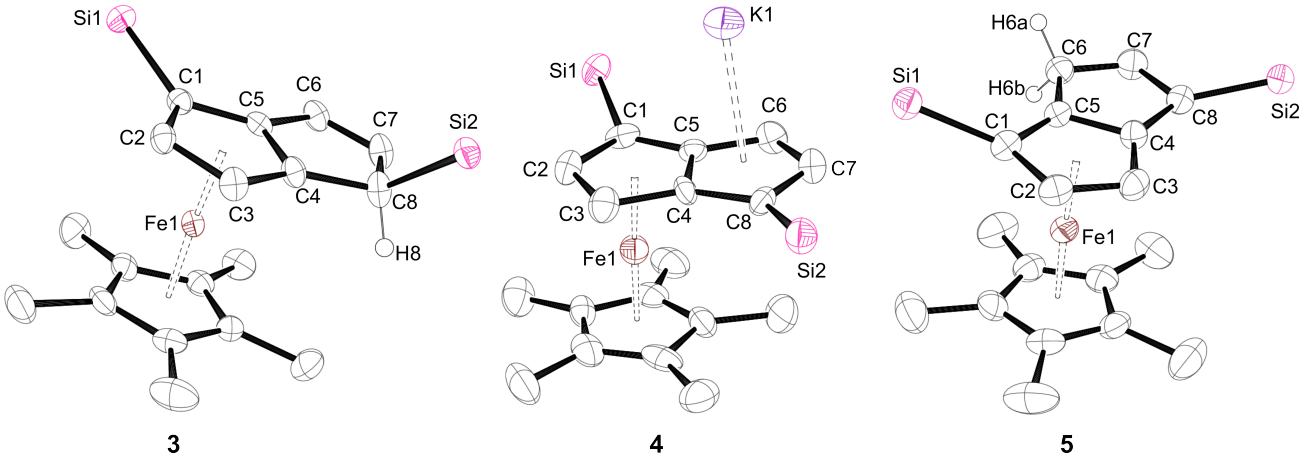

Fig. 5. Displacement ellipsoid plots (50% probability) of **3**, **4** and **5**. Hydrogen atoms (except allylic H's) and ^{i}Pr groups omitted for clarity.

Table 2. Selected distances (Å), angles (°) and parameters (Fig. 4) for **3**, **4** and **5**. Ct1 and Ct3 correspond to the η^5-centroids of Pn and Cp* rings respectively.

Parameter	**3**	**4**	**5**
Fe–C1	2.101(3)	2.088(4)	2.079(3)
Fe–C2	2.043(3)	2.014(4)	2.029(3)
Fe–C3	2.050(3)	2.052(4)	2.057(3)
Fe–C4	2.079(3)	2.183(4)	2.136(3)
Fe–C5	2.069(3)	2.135(4)	2.091(3)
$\Delta_{\text{Fe-Ct1}}$	0.009	0.108	0.059
Fe–Ct1	1.6700(16)	1.6937(18)	1.6799(18)
Fe–Ct3	1.6667(17)	1.6468(18)	1.701(2)
Ct1–Fe–Ct3	175.53(6)	173.91(11)	176.56(8)
C1–C2	1.446(4)	1.457(6)	1.455(4)
C2–C3	1.426(4)	1.436(6)	1.419(5)
C6–C7	1.350(4)	1.393(6)	1.420(4)
C7–C8	1.504(4)	1.432(6)	1.409(4)
av. C–C_{ring}	1.443(4)	1.440(6)	1.436(5)
C2–C1–Si1	122.2(2)	121.2(3)	125.0(2)

C7–C8–Si2	113.3(3)	122.4(3)	123.1(3)
Fe···K	-	4.834	-

The K atom is closer to the Pn† ring in **4** than in **2**, such that it should not be considered as a charge separated heterobimetallic. Interestingly, the K atom also has close interactions with the Cp* ring of another molecule in the lattice, with K–C distances in the range 3.077(4) - 3.285(4) Å. An extended ellipsoid plot (Fig.6) shows that **4** is an organometallic polymer in the solid state.

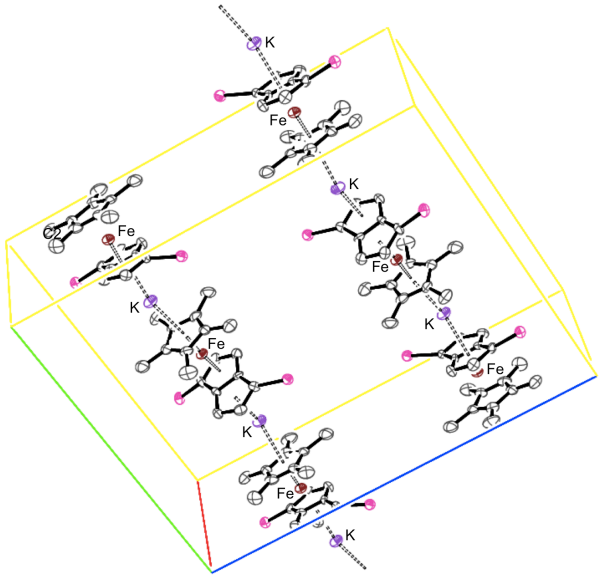

Fig. 6. ORTEP view of the unit cell of **4** (50% ellipsoids).
H atoms and ^{i}Pr groups removed for clarity.

Synthesis and characterisation of [FeCp]$_2$(μ:η^5,η^5-Pn†) (**6**)*

Despite its extreme sensitivity, Fe/K complex **4** presents a potentially useful precursor for other Fe/M anti-bimetallics or for introducing additional substituents to the Pn† ligand. As an initial proof of concept, the synthesis of the homonuclear bimetallic [Cp*Fe]$_2$(μ:η^5,η^5-Pn†) (**6**) from **4** was attempted.

To a solution of **4** in THF-d_8 was added one equivalent of Cp*FeCl(TMEDA) and a colour change to brown was observed after 4 h with the appearance of a brown solid. ^{1}H NMR spectroscopy of the filtrate showed complete disappearance of the four aromatic signals of **4**, and appearance of two new doublets at 4.67 and 3.69 ppm, assigned to **6** in *ca.* 40% conversion by relative integration. Additional products identified by ^{1}H NMR were Cp*Fe(η^5-Pn†H) isomers **3** and **5** resulting from adventitious protonation of **4**. The homonuclear bimetallic complex **6** was independently synthesised in a single step

by reaction of two equivalents of Cp*FeCl(TMEDA) with $[K]_2Pn^{\dagger}$ in THF (Scheme 7, bottom), and isolated after work-up as dark green crystals in 34% yield.

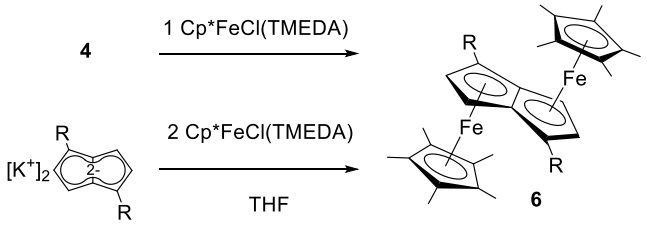

Scheme 7. Synthetic routes to **6**. R = Si^iPr_3.

Analytical and spectroscopic measurements were consistent with the proposed formulation of **6**, and the molecular structure of **6** was confirmed by a single crystal XRD study (Fig. 7). **6** was poorly soluble in aliphatic and aromatic hydrocarbons and polar solvents (MeCN, ^{t}BuOMe, and Et_2O) at room temperature, despite the precedent for improved solubility of complexes with Si^iPr_3 substituted pentalene ligands.[30] However, **6** was sufficiently soluble in THF-d_8 for its ^{1}H NMR to be identified and allowed for its electrochemistry to be studied in this solvent. Multinuclear (^{1}H, ^{13}C, ^{29}Si) NMR spectra of **6** were consistent with a centrosymmetric structure on the NMR timescale. The $Pn^{\dagger}$ ligand exhibits metallocene-like μ-η^5:η^5 coordination of the two metal centres in **6**, but with the Fe atoms more distant from the bridgehead carbon atoms (C4 and C4') than the three wingtip carbons (C1, C2 and C3), as quantified by the large ring-slippage (Δ, defined in Fig. 4) value of 0.128 Å for this complex. A similar slipping distortion has been reported in several indenyl-[31] and pentalenyl-[10,23] metal complexes. This has been attributed in the latter to a maximisation of interaction of the metal with the π-electron density of the fused ring system, which is delocalised around its perimeter. Homobimetallic **6** shows the longest average C–C ring distances (1.454(4) Å) of the complexes reported herein, and in general a smaller range of ring C–C distances are found in those complexes bearing the aromatic $Pn^{\dagger}$ ligand. For comparison the ring C–C distances in Fe/K hetero-bimetallic complexes **2** and **4** are intermediate between these extremes of 'aromatic' and 'localised' character.

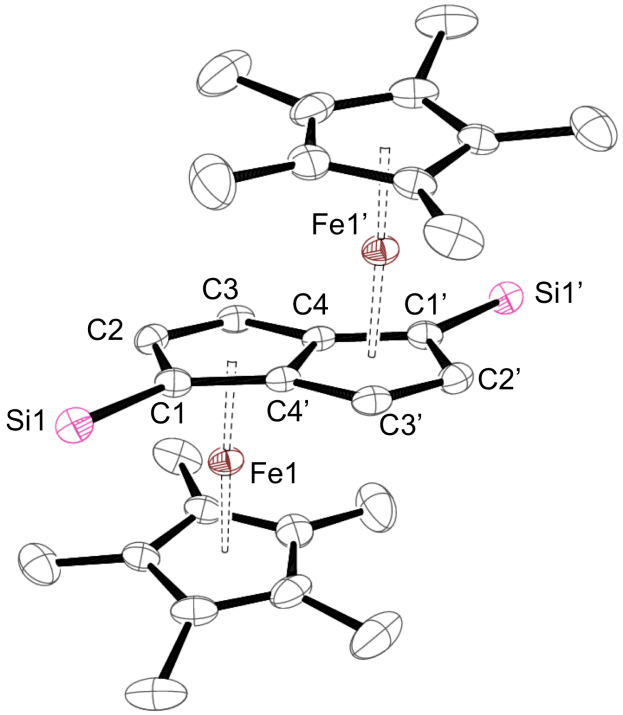

Fig. 7. Displacement ellipsoid plot (50% probability) of **6**. Hydrogen atoms and ^{i}Pr groups omitted for clarity. Primed atoms are generated by symmetry.

Table 3. Selected distances (Å), angles (°) and parameters (Fig. 4) for **6**. Ct1 and Ct3 are the η^5-centroids of the Pn and Cp* rings respectively.

Parameter	**6**	**Parameter**	**6**
Fe–C1	2.123(3)	Fe–Ct1	1.7193(13)
Fe–C2	2.033(3)	Fe–Ct3	1.7064(13)
Fe–C3	2.045(3)	Ct1–Fe–Ct3	173.36(7)
Fe–C4	2.195(3)	C1–C2	1.456(4)
$\Delta_{\text{Fe-Ct1}}$	0.128	C2–C3	1.425(4)
Fe···Fe	4.132	C2–C1–Si1	125.4(2)

Towards oligomeric pentalene-bridged complexes

Following the successful synthesis of **6**, the same methodology was employed in the attempted synthesis of heteronuclear 3*d*/4*s* pentalene complexes, Cp*Fe(μ-Pn†)LnCp* (Ln = Yb, Sm). As a general procedure, a THF solution of **4** was prepared *in situ* and treated with one equivalent (per Ln) of half-sandwich complexes [Cp*Ln(μ-I){THF}]$_2$ or Cp*Ln(BPh$_4$). The reaction mixture was then filtered and analysed by ^{1}H NMR spectroscopy and mass spectrometry. In each case, monometallic Cp*Fe(η^5-Pn†H) isomers **3** and **5** were the sole products identified in the ^{1}H NMR spectra, and EI-MS showed a parent ion at *m/z* = 607 (100%) with no higher peaks assignable to bimetallic complexes.

Electrochemical Studies

The electrochemistry of the Fe(II) complexes in THF was studied by cyclic voltammetry (CV) to gain insight into the electron donating properties of silylated pentalene ligands, and their ability to delocalise charge over two metal centres in anti-bimetallic complexes. The use of [^{n}Bu$_4$N][B(C$_6$F$_5$)$_4$] as the supporting electrolyte resulted in better resolution CV data compared with [^{n}Bu$_4$N][PF$_6$], due to its lower ion-pairing capabilities (spherical diameter [B(C$_6$F$_5$)$_4$]$^-$ = 10 Å; [PF$_6$]$^-$ = 3.3 Å)[32] which is beneficial for the study of multi-electron processes with positively charged analytes.[33]

Complexes **1** and **3** each showed a single redox process assigned to the Fe(III)/Fe(II) couple (actual voltammograms are presented in the ESI). Repetitive potential cycling over electrochemical events revealed that the voltammetric responses for the oxidative and reductive waves are stable, while varying the scan rate again revealed that the voltammetry was under diffusion control and that no fouling or adsorption onto the electrode surface was occurring. In each case the ratio of oxidative and reductive peak currents (i_{pa}/i_{pc}) is close to unity, signifying a quasi-reversible process. The peak-to-peak separation (ΔE_{pp}) is comparable to that for ferrocene under the same conditions (*ca.* 100 mV), showing that only one electron is being transferred. The ideal ΔE_{pp} for a fully reversible single electron transfer at 298 K is 59 mV,[34] however this discrepancy is attributed to Ohmic losses (*iR* drop) in THF rather than sluggish electron transfer kinetics.

The mid-peak potential ($E_{½} = \{E_{pa} + E_{pc}\}/2$) of substituted ferrocene complexes shift to more negative values as the electron donor properties of the ligand increases.[35,36] For example the $E_{½}$ of decamethylferrocene under these conditions is -0.52 V (vs $FeCp_2^{+/0}$, a convention which is assumed for all potentials quoted henceforth),[32] due to the electron donating (+I effect) of the methyl substituents

on the Cp* ring. The $E_{½}$ for **1** and **3** are -0.21 and -0.42 V respectively, implying that the electron donating properties of the η^5- ligands to the Fe(II) centre increases in the sequence Cp < $Pn^{\dagger}H$ < Cp* (Table 4). In this context the η^5-$Pn^{\dagger}H$ ligand can be viewed as one cyclopentadienyl ring with one silyl and two alkyl substituents, leading to an increased +I effect with respect to Cp.

The electrochemistry of **4** was of interest in terms of the bonding in the anionic [Cp*Fe(η^5-$Pn^{\dagger}$)]$^-$ fragment, for comparison with the DFT calculations on model systems.[37] The CV of **4** (Fig. 8) shows two quasi-reversible one electron processes at -1.88 and -0.35 V, which could possibly be assigned to purely metal based Fe^{II}/Fe^{III} and Fe^{III}/Fe^{IV} processes but DFT calculation (see below) suggest successive oxidations from an orbital that has both metal and ligand character.

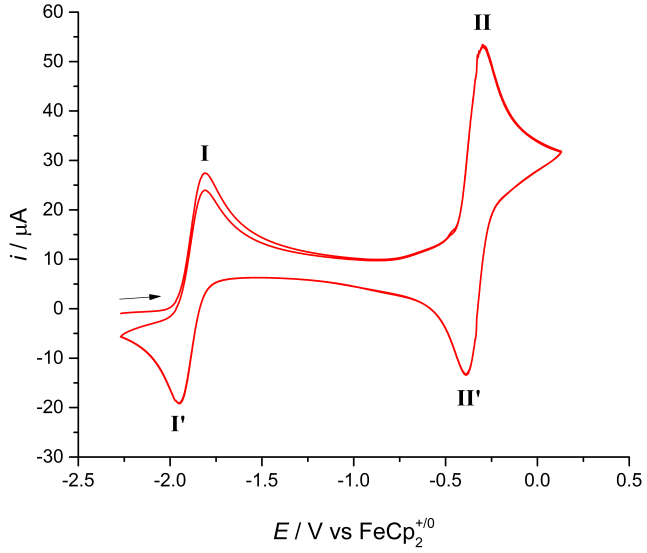

Fig. 8. Overlaid CV scans (2 cycles) for **4** in THF / 50 mM [^{n}Bu$_4$N][B(C$_6$F$_5$)$_4$], scan rate 100 mV s^{-1}.

Table 4. Electrode potentials ($E_{½}$) vs $FeCp_2^{+/0}$ in THF / 50 mM [^{n}Bu$_4$N][B(C$_6$F$_5$)$_4$].

Compound	$E_{½}$ / V	ref
Fe(η^5-$Pn^{\dagger}H$)$_2$ (**1**)	-0.28	this work
Cp*Fe(η^5-$Pn^{\dagger}H$) (**3**)	-0.41	this work
FeCp*$_2$	-0.52	[32]
[Cp*Fe(η^5-$Pn^{\dagger}$)][K] (**4**)	(I) -1.88 (II) -0.35	this work
[Cp*Fe]$_2$(μ-$Pn^{\dagger}$) (**6**)	(I) -0.80[a] (II) -0.35	this work

$[Cp^*Fe]_2(\mu\text{-Pn})$	(I) -0.84 (II) -0.51	[7], this work

[a] Irreversible anodic process

CV allows an initial investigation into the stability of the mixed-valence states in bimetallic complexes e.g. $[Fe^{II}–Fe^{III}]^+$, and enables the appropriate chemical redox agent to be chosen for their large-scale preparation. The CV of **6** (Fig. 9) shows an irreversible oxidation peak at $E_{pa}^{(I)} = -0.80$ V and a quasi-reversible process centered at $E_{½}^{(II)} = -0.35$ V. These results suggest that the mixed valence species $[\mathbf{6}]^+$ is not stable under the conditions and timescale of the experiment, and hence the isolation of $[\mathbf{6}]^+$ was not pursued. The unsubstituted pentalene analogue $[Cp^*Fe]_2(\mu\text{-Pn})$ was synthesised for comparison,[7] and its CV in this solvent/electrolyte system shows two quasi-reversible processes with a potential difference ($\Delta E_{½}$) of 0.33 V, consistent with a strong electronic interaction between the Fe centres and extensive delocalisation in the mixed-valence state.

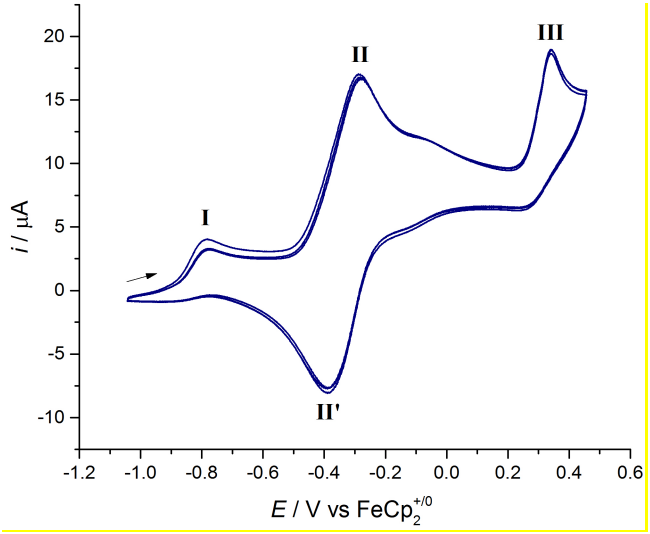

Fig. 9. Overlaid CV scans (2 cycles) for **6** in THF / 50 mM $[^nBu_4N][B(C_6F_5)_4]$, scan rate 100 mV s^{-1}.

DFT Calculations

Electronic structure calculations were carried out on a series of FePnCp derivatives. Geometries were optimized using C_s symmetry for $[CpFe(\eta^5\text{-Pn})]^-$, $[CpFe(\eta^5\text{-Pn})]K$, $[Cp^*Fe(\eta^5\text{-Pn})]^-$ and $[Cp^*Fe(\eta^5\text{-Pn})]K$, one interest being the charge carried by the uncoordinated C atoms of the pentalene ligand. The deprotonated complex **4** was found to be unsuitable for the synthesis of heterobimetallic Fe/Ln

pentalene complexes *via* salt metathesis reactions with Cp*Ln(II) reagents. This may be rationalised by inspecting the DFT structure of unsubstituted analogue $[CpFe(\eta^5\text{-}Pn)]^-$, reported by Saillard *et al*.[37] The net charges on the uncomplexed part of the pentalene ring in this model complex do not show any significant carbanionic character (Fig. 10), which is consistent with it being less nucleophilic at these positions. However, calculated charges are method dependent;[38] Saillard *et al*. employed Mulliken charges.[37] Table 5 gives the charges on C6, C7 and C8 of the Pn ligand estimated by three methods, namely Mulliken,[39] Hirshfeld[40] and Voronoi,[41] for the four complexes studied.

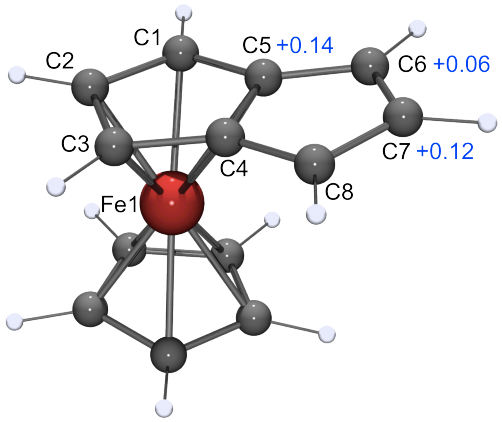

Fig. 10. Ball and stick diagram of calculated structure of $[CpFe(\eta^5\text{-}Pn)]^-$ constructed from coordinates published by Saillard *et al*.[37] Labelling system for the Pn ligand shown in black and net charges on C atoms in blue.

Table 5. Selected atomic charge densities for DFT optimized structures.

Structure	Atoms	Mulliken charge	Hirshfeld	Voronoi
$[CpFe(\eta^5\text{-Pn})]^-$	C6, C8	0.056	-0.153	-0.149
	C7	0.124	-0.120	-0.091
$[CpFe(\eta^5\text{-Pn})]K$	C6, C8	0.005	-0.144	-0.156
	C7	0.088	-0.107	-0.096
$[Cp^*Fe(\eta^5\text{-Pn})]^-$	C6, C8	-0.50	-0.148	-0.148
	C7	0.122	-0.115	-0.091
$[CpFe(\eta^5\text{-Pn})]K$	C6, C8	-0.009	-0.142	-0.157
	C7	0.082	-0.104	-0.096
$[Cp^*Fe(\eta^5\text{-Pn})]^-$	Fe	0.312	0.020	-0.075
$[Cp^*Fe(\eta^5\text{-Pn})]$	Fe	0.265	0.079	-0.026
$[Cp^*Fe(\eta^5\text{-Pn})]^+$	Fe	0.203	0.112	-0.003

The Hirshfeld and Voronoi analyses give negative charges on C6–C8 for all four complexes. All methods suggest that the charges on these atoms are relatively insensitive to the methylation of the cyclopentadienyl ring or to the presence of a potassium ion. The results indicate that the lack of negative charge on the pentalene is not the reason for failed synthesis of a lanthanide bimetallic derivative, rather the steric bulk of the Si^iPr_3 groups hinder coordination.

It was also of interest to examine the nature of the two reversible oxidations shown for **4** by CV. To this end the geometries of $[Cp^*Fe(\eta^5\text{-Pn})]$ and $[Cp^*Fe(\eta^5\text{-Pn})]^+$ were optimized. Both singlet and triplet states were considered for the cation but the singlet state was found to be the more stable. The HOMO of $[Cp^*Fe(\eta^5\text{-Pn})]^-$ has approximately equal ligand:metal character (Fig. 11). The uncoordinated ring resembles the 'allyl' functionality of Pn and has an out-of-phase interaction with the d_{xy} orbital of Fe.

This suggests a repulsive interaction between Fe and the uncoordinated allyl fragment, which is consistent with the larger ring slippage in the molecular structure of **4** relative to **3** (Δ = 0.108 and 0.009 respectively). For the neutral species one electron was removed from this orbital and for the cation it constituted the LUMO of the molecule. The ring slippage was reduced on successive oxidation of the [Cp*Fe(η^5-Pn)] anionic, neutral and cationic species (Δ = 0.046, 0.018 and -0.003 Å respectively). The charges on the Fe atom for the anionic, neutral and cationic species are listed in Table 5. Rather counter intuitively the Mulliken charge on Fe decreases with successive oxidation. A more realistic picture is given by the Hirshfeld and Voronoi charges, which show small successive shifts to a more positive Fe atom on oxidation. Overall each oxidation involves removal of electron density from both metal and ligands.

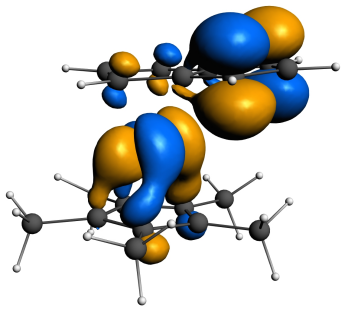

Fig. 11. Isosurfaces for the HOMO of [Cp*Fe(η^5-Pn)]$^-$.

It must be emphasised that these DFT modelled structures do not take into account the Si^{i}Pr$_3$ substituent on the uncoordinated ring in **4**, which is likely to obstruct the approach of a large Cp*Ln(II) electrophile. Furthermore **4** exists as an oligomer in the solid state and if this structure persists to some extent in solution, it may provide an additional kinetic barrier to substitution reactions with Cp*LnX.

CONCLUSIONS

In these studies towards oligomeric and heteronuclear organometallic complexes, a total of six new Fe(II) compounds incorporating silylated pentalene ligands have been synthesised and characterised. A combination of NMR spectroscopic and single crystal XRD methods were used to elucidate the different isomers that form in the case of the homoleptic Pn†H complex **1**. Subsequent synthetic studies showed that **1** could be singly deprotonated to form the mono-potassium salt **2**, however the latter was unsuitable as a synthon for incorporating further metal fragments into the chain, and instead underwent

decomposition reactions to afford a mixture of isomers. The mixed-sandwich $Pn^{\dagger}H$/Cp* complex **3**, formed as a single isomer**,** was synthesised as a more symmetrical precursor to trimetallic and heteronuclear complexes. Complex **3** could also be deprotonated to form potassium salt **4**, which shows an intriguing polymeric structure in the solid state. Compound **4** was utilised in the stepwise synthesis of homonuclear bimetallic **6**, but ultimately **4** also proved unsuitable for the synthesis of trimetallic or heterobimetallic Fe-Ln(II) complexes, and ligand protonation occurred to form complexes **3** and **5**. DFT studies on model mono-Fe complexes revealed that the uncoordinated C atoms of the pentalene ligand carry a net negative charge, and hence the observed reactivity is attributed to the steric bulk of the $Si^{i}Pr_3$ substituents.

Cyclic voltammetry was used to quantify the relative electron donating ability of the η^5- ligands to the Fe(II) centre, and $Pn^{\dagger}H$ was found to be more electron donating than Cp but less than Cp* ligands. CV of the anion **4** revealed two quasi-reversible processes, suggesting the oxidation products have some stability on the experimental timescale. Geometry optimized structures for $[Cp^*FePn]^0$ and $[Cp^*FePn]^+$ were calculated using DFT, and MO analysis suggests the oxidation of $[Cp^*FePn]^-$ occurs from orbitals that have both metal and ligand character. The difference in redox potentials between centres bridged by the $Pn^{\dagger}$ ligand in **6** was of a similar order to that of found by Manriquez *et al.* using Pn, however the first oxidation process for **6** was irreversible.

EXPERIMENTAL

General procedures

All manipulations were carried out using standard Schlenk techniques under Ar, or in an MBraun glovebox under N_2 or Ar. All glassware was dried at 160 °C overnight prior to use. Solvents were purified by pre-drying over sodium wire and then distilled over Na (toluene, TMEDA), K (THF, hexane, ^{t}BuOMe) or Na-K alloy (Et_2O, pentane) under a N_2 atmosphere. Dried solvents were collected, degassed and stored over argon in K mirrored ampoules, except THF, Et_2O and TMEDA which were stored in ampoules containing activated 4 Å molecular sieves. Deuterated solvents were degassed by three freeze−pump−thaw cycles, dried by refluxing over K for 3 days, vacuum distilled into ampoules and stored under N_2. The compounds $Pn^{\dagger}H_2$, $[K]_2Pn^{\dagger}$,[42] $[K]Pn^{\dagger}H$,[6] Cp*FeCl(TMEDA),[43] KBn,[44] and $FeCp^*_2$[45] were prepared according to published procedures. Microanalysis of $FeCl_2(THF)_x$[46] was carried out to determine the amount of coordinated THF, and the data obtained best fit to a value of $x = 1.1$. Reagents Bu_2Mg, KH, $[^{n}Bu_4N][B(C_6F_5)]$, YbI_2 and $Ca(N\{SiMe_3\}_2)_2$ were

kindly donated by co-workers. NMR spectra were measured on Varian VNMRS 400 (^{1}H 399.5 MHz; ^{13}C{^{1}H} 100.25 MHz; ^{29}Si{^{1}H} 79.4 MHz) or VNMRS 500 (^{1}H 499.9 MHz; ^{13}C{^{1}H} 125.7 MHz) spectrometers. The spectra were referenced internally to the residual protic solvent (^{1}H) or the signals of the solvent (^{13}C). ^{29}Si{^{1}H} NMR spectra were referenced externally relative to $SiMe_4$. IR spectra were recorded between NaCl plates using a Perkin-Elmer Spectrum One FTIR instrument. Mass spectra were recorded using a VG Autospec Fisons instrument (EI at 70 eV). Elemental analyses for were carried out at the Elemental Analysis Service, London Metropolitan University. Cyclic voltammetry studies were carried out using a BASi Epsilon-EC potentiostat under computer control. *iR* drop was compensated by the feedback method. CV experiments were performed in an Ar glovebox using a three-electrode configuration with a Au disc (2.0 mm^2) or glassy carbon disc (7.0 mm^2) as the working electrode, a Pt wire as the counter electrode and a Ag wire as the pseudo-reference electrode. Sample solutions were prepared by dissolving the analyte (*ca.* 5 mM) in THF (1.0 cm^3) followed by addition of a supporting electrolyte [^{n}Bu$_4$N][B(C$_6$F$_5$)] or [^{n}Bu$_4$N][PF$_6$]. The reported mid-peak potentials are referenced internally to that of the $FeCp_2^{+/0}$ redox couple, which was measured by adding ferrocene (*ca*. 1 mg) to the sample solution.

Syntheses

*Synthesis of Fe(η^5-Pn†H)$_2$ (**1**)*

[K]Pn†H (1.60 g, 3.37 mmol) in THF (20 mL) was added dropwise to a suspension of $FeCl_2(THF)_{1.1}$ (0.45 g, 2.18 mmol) in THF (20 mL) while stirring at -78 °C; the resulting mixture was then allowed to warm to room temperature and stirred overnight. The volatiles were removed under reduced pressure, and the products extracted into pentane (3 x 20 mL) and filtered through Celite. The filtrate was stripped to dryness to afford a crude red solid. **1** was recrystallised from a saturated Et_2O (20 mL) solution at -50 °C as dark red crystals which were washed with pentane at -78 °C and dried *in vacuo***.** Yield: 1.26 g (65% with respect to $FeCl_2(THF)_{1.1}$).

Major isomer ^{1}H NMR (C$_6$D$_6$, 399.5 MHz, 303 K): δ_H 6.63 (2H, dd, $^3J_{HH}$ = 5.3, 2.2 Hz, Pn vinylic *H*), 6.51 (2H, dd, $^3J_{HH}$ = 5.3, $^4J_{HH}$ = 1.6 Hz, Pn vinylic *H*), 4.01 (2H, d, $^3J_{HH}$ = 1.8 Hz, Pn aromatic *H*), 3.93 (2H, d, $^3J_{HH}$ = 1.8 Hz, Pn aromatic *H*), 3.58 (2H, apparent t, $^3J_{HH}$ = 2.2 Hz, Pn allylic *H*), 1.36 (12H, m, ^{i}Pr C*H*), 1.29 (18H, br, ^{i}Pr C*H*$_3$), 1.27 (18H, d, $^3J_{HH}$ = 7.1 Hz, ^{i}Pr C*H*$_3$), 1.14 (18H, br, ^{i}Pr C*H*$_3$), 1.04 (18H, br, ^{i}Pr C*H*$_3$). ^{13}C{^{1}H} NMR (C$_6$D$_6$, 100.5 MHz, 303 K): δ_C 138.48 (Pn vinylic *C*), 129.80 (Pn vinylic *C*), 102.76 (Pn bridgehead *C*), 99.42 (Pn bridgehead *C*), 78.46 (Pn aromatic *C*), 68.99 (Pn aromatic *C*), 59.99 (Pn aromatic *C*-Si), 36.20 (Pn allylic *C*), 19.78 (^{i}Pr *C*H), 19.73 (^{i}Pr *C*H), 19.54 (^{i}Pr

*C*H), 19.29 (^{i}Pr *C*H), 12.68 (^{i}Pr *C*H$_3$), 12.04 (^{i}Pr *C*H$_3$). ^{29}Si{^{1}H} NMR (C$_6$D$_6$, 79.4 MHz, 303 K): δ_{Si} 5.50 (allylic *Si*), 5.22 (aromatic *Si*).

Minor isomer ^{1}H NMR (C$_6$D$_6$, 399.5 MHz, 303 K): δ_{H} 6.59 (2H, dd, $^{3}J_{HH}$ = 5.2, $^{4}J_{HH}$ = 1.1 Hz, Pn vinylic *H*) 6.22 (2H, dd, $^{3}J_{HH}$ = 5.2, 2.3 Hz, Pn vinylic *H*), 4.20 (2H, d, $^{3}J_{HH}$ = 1.7 Hz, Pn aromatic *H*), 4.14 (2H, d, $^{3}J_{HH}$ = 1.7 Hz, Pn aromatic *H*), 2.29 (2H, apparent t, $^{3}J_{HH}$ = 2.2 Hz, Pn allylic *H*), 1.36 (12H, m, ^{i}Pr C*H*), 1.31 (18H, br, ^{i}Pr C*H*$_3$), 1.26 (18H, d, $^{3}J_{HH}$ = 7.1 Hz, ^{i}Pr C*H*$_3$), 1.10 (18H, br, ^{i}Pr C*H*$_3$), 1.03 (18H, br, ^{i}Pr C*H*$_3$). ^{13}C{^{1}H} NMR (C$_6$D$_6$, 100.5 MHz, 303 K): δ_{C} 137.36 (Pn vinylic *C*), 125.88 (Pn vinylic *C*), 102.03 (Pn bridgehead *C*), 98.26 (Pn bridgehead *C*), 78.13 (Pn aromatic *C*), 64.68 (Pn aromatic *C*), 59.53 (Pn aromatic *C*-Si), 26.51 (Pn allylic *C*), 19.62 (^{i}Pr *C*H), 19.45 (^{i}Pr *C*H), 19.20 (^{i}Pr *C*H), 12.75 (^{i}Pr *C*H$_3$), 12.27 (^{i}Pr *C*H$_3$). ^{29}Si{^{1}H} NMR (C$_6$D$_6$, 79.4 MHz, 303 K): δ_{Si} 5.67 (allylic *Si*), 4.58 (aromatic *Si*). EI-MS: *m/z* = 887 (100%), [M]$^{+}$. Anal. found (calcd. for C$_{52}$H$_{94}$FeSi$_4$): C, 70.48 (70.37); H, 10.60 (10.68) %.

*Synthesis of (η^5-Pn†H)Fe[η^5-Pn†(η^5-K{THF}$_2$)] (**2**)*

Pre-cooled THF (-78 °C, 20 mL) was added to an ampoule containing a solid mixture of **1** (48 mg, 0.07 mmol) and KNH_2 (8 mg, 0.14 mmol) at -78 °C. The resulting suspension was stirred at -78 °C for 30 min, then allowed to warm to room temperature and stir for 12 h yielding a red-green solution. The volatiles were removed under reduced pressure and the resulting solids extracted into pentane (20 mL) and filtered. Concentration of the filtrate and subsequent cooling to -50 °C yielded dark red crystals of **2** suitable for single crystal XRD analysis. Yield: 39 mg (52% with respect to **1**).

^{1}H NMR (THF-d_8, 399.5 MHz, 303 K, selected data): δ_{H} 6.92 (1H, br s, Pn *H*), 6.81 (1H, d, $^{3}J_{HH}$ = 3.4 Hz, Pn *H*), 6.58 (1H, d, $^{3}J_{HH}$ = 3.7 Hz, Pn *H*), 5.48 (1H, d, $^{3}J_{HH}$ = 3.7 Hz, Pn *H*), 5.39 (1H, br d, $^{3}J_{HH}$ = 3.6 Hz, Pn *H*), 5.22 (1H, d, $^{3}J_{HH}$ = 3.4 Hz, Pn *H*), 4.74 (1H, br s, Pn *H*), 4.39 (1H, br d, $^{3}J_{HH}$ = 1.6 Hz, Pn *H*), 3.41 (1H, br d, $^{3}J_{HH}$ = 2.0 Hz, Pn *H*), 1.37 (12H, m, ^{i}Pr C*H*), 1.23 (18H, d, $^{3}J_{HH}$ = 7.4 Hz, ^{i}Pr C*H*$_3$), 1.00 (18H, d, $^{3}J_{HH}$ = 7.4 Hz, ^{i}Pr C*H*$_3$), 0.97 (18H, d, $^{3}J_{HH}$ = 7.5 Hz, ^{i}Pr C*H*$_3$), 0.93 (9H, d, $^{3}J_{HH}$ = 7.3 Hz, ^{i}Pr C*H*$_3$). ^{13}C{^{1}H} NMR (THF-d_8, 100.5 MHz, 303 K, selected data): δ_{C} 138.2 (Pn *C*), 132.8 (Pn *C*), 122.1 (Pn *C*), 100.5 (Pn *C*), 98.79 (Pn *C*), 78.18 (Pn *C*), 75.51 (Pn *C*), 73.86 (Pn *C*), 71.27 (Pn *C*), 54.24 (Pn *C*), 43.20 (Pn *C*), 19.74 (^{i}Pr *C*H$_3$), 19.72 (^{i}Pr *C*H$_3$), 19.69 (^{i}Pr *C*H$_3$), 19.64 (^{i}Pr *C*H$_3$), 19.57 (^{i}Pr *C*H$_3$), 19.55 (^{i}Pr *C*H$_3$), 19.49 (^{i}Pr *C*H$_3$), 19.44 (^{i}Pr *C*H$_3$), 13.04 (^{i}Pr *C*H), 13.01 (^{i}Pr *C*H), 12.98 (^{i}Pr *C*H), 12.83 (^{i}Pr *C*H). ^{29}Si{^{1}H} NMR (THF-d_8, 79.4 MHz, 303 K, selected data): δ_{Si} 8.53, -2.74. EI-MS: No volatility. Anal. found (calcd. for C$_{60}$H$_{107}$FeKO$_2$Si$_4$): C, 70.48 (67.49); H, 10.60 (10.10) %.

*Synthesis of Cp*Fe(η^5-Pn†H) (**3**)*

[K]Pn†H (4.35 mmol) in THF (30 mL) was added dropwise to a green solution of FeCp*Cl(TMEDA) (1.492 g, 342.7 mmol) in THF (20 mL) at -78 °C, and allowed to warm to room temperature overnight. The resulting red suspension was stripped of solvent, and the products extracted into hexane (100 mL) and filtered through Celite on a frit. The solvent was removed under reduced pressure to afford a crude orange solid. **6** was recrystallised from a saturated Et_2O (40 mL) solution at -20 °C as orange-red blocks which were washed with pentane at -78 °C and dried *in vacuo*. A second crop of crystals was obtained from slow cooling the combined supernatant and washings to -50 °C. Total yield: 1.58 g (81% with respect to [K]Pn†H).

^{1}H NMR (C_6D_6, 499.9 MHz, 303 K): δ_H 6.49 (1H, dd, $^3J_{HH}$ = 5.4, 2.1 Hz, Pn vinylic *H*), 6.43 (1H, dd, $^3J_{HH}$ = 5.4, $^4J_{HH}$ = 1.7 Hz, Pn vinylic *H*), 3.79 (1H, d, $^3J_{HH}$ = 2.1 Hz, Pn aromatic *H*), 3.67 (1H, d, $^3J_{HH}$ = 1.9 Hz, Pn aromatic *H*), 3.26 (1H, apparent t, $^3J_{HH}$ = 2.1 Hz, Pn allylic *H*), 1.74 (15H, s, Cp* C*H*$_3$), 1.39 (3H, m, ^{i}Pr C*H*), 1.27 (9H, d, $^3J_{HH}$ = 7.4 Hz, ^{i}Pr C*H*$_3$), 1.25 (9H, d, $^3J_{HH}$ = 7.4 Hz, ^{i}Pr C*H*$_3$), 1.20 (3H, m, ^{i}Pr C*H*), 1.14 (9H, br, ^{i}Pr C*H*$_3$), 1.08 (9H, br, ^{i}Pr C*H*$_3$). ^{13}C{^{1}H} NMR (C_6D_6, 125.7 MHz, 303 K): δ_C 135.85 (Pn vinylic *C*), 129.05 (Pn vinylic *C*), 102.34 (Pn bridgehead *C*), 98.50 (Pn bridgehead *C*), 80.77 (Pn aromatic *C*), 78.27 (Cp*-*C*CH$_3$), 68.75 (Pn aromatic *C*), 61.20 (Pn aromatic *C*-Si), 32.68 (Pn allylic *C*), 19.78 (^{i}Pr *C*H), 19.68 (^{i}Pr *C*H), 19.57 (^{i}Pr *C*H), 19.39 (^{i}Pr *C*H), 12.42 (^{i}Pr *C*H$_3$), 12.09 (^{i}Pr *C*H$_3$), 10.69 (Cp* *C*H$_3$). ^{29}Si{^{1}H} NMR (C_6D_6, 79.4 MHz, 303 K): δ_{Si} 5.62 (allylic *Si*), 5.57 (aromatic *Si*). EI-MS: *m/z* = 607 (100%), [M]$^+$. Anal. found (calcd. for $C_{36}H_{62}FeSi_2$): C, 71.15 (71.25); H, 10.25 (10.30) %.

*Synthesis of [Cp*Fe(η^5-Pn†)][K] (**4**)*

An ampoule was charged with **3** (107 mg, 0.18 mmol) and KNH_2 (19 mg, 0.80 mmol) to which was added THF (20 mL). The mixture was stirred for 4 days yielding a dark red suspension. Filtration on a frit through dry Celite yields a red solution containing **4** in approx. quantitative yield by NMR spectroscopy. The volatiles were removed under reduced pressure and the resulting residue extracted into Et_2O (10 mL). Storage of this solution at -35 °C yielded dark red crystals of **4** suitable for X-ray diffraction. Yield: 85 mg (75% with respect to **3**).

^{1}H NMR (C_6D_6 / THF-d_8, 499.9 MHz, 303 K): δ_H 7.33 (1H, d, $^3J_{HH}$ = 3.7 Hz, Fe-Pn C*H*), 5.65 (1H, d, $^3J_{HH}$ = 3.7 Hz, Fe-Pn wingtip C*H*), 4.14 (1H, d, $^3J_{HH}$ = 2.0 Hz, K-Pn C*H*), 3.35 (1H, d, $^3J_{HH}$ = 2.0 Hz, K-Pn wingtip C*H*), 1.84 (15H, s, Cp* C*H*$_3$), 1.54 (3H, overlapping m, ^{i}Pr C*H*), 1.46 (3H, overlapping m, ^{i}Pr C*H*), 1.41 (9H, d, $^3J_{HH}$ = 7.4 Hz, ^{i}Pr C*H*$_3$), 1.36 (9H, d, $^3J_{HH}$ = 7.4 Hz, ^{i}Pr C*H*$_3$), 1.35 (9H, br, ^{i}Pr

CH_3), 1.33 (9H, br, ^{i}Pr CH_3). ^{13}C{^{1}H} NMR (C_6D_6 / THF-d_8, 125.7 MHz, 303 K): δ_C 138.28 (Fe-Pn *C*H), 110.53 (Pn bridgehead *C*), 98.91 (Pn bridgehead *C*), 93.66 (Fe-Pn wingtip *C*H), 76.88 (Fe-Pn *C*-Si), 76.53 (K-Pn *C*H), 76.10 (Cp*-*C*CH$_3$), 61.25 (K-Pn wingtip *C*H), 48.18 (K-Pn *C*-Si), 20.60 (^{i}Pr *C*H$_3$), 20.54 (^{i}Pr *C*H$_3$), 20.36 (^{i}Pr *C*H$_3$), 20.33 (^{i}Pr *C*H$_3$), 14.67 57 (^{i}Pr *C*H), 13.86 57 (^{i}Pr *C*H), 11.22 (Cp* *C*H$_3$). ^{29}Si{^{1}H} NMR (C_6D_6, 79.4 MHz, 303 K): δ_{Si} 5.60 (Fe-Pn *Si*), -5.98 (K-Pn *Si*). EI-MS: *m/z* = 607 (100%), [M - K + H]$^+$. Anal. found (calcd. for $C_{36}H_{61}FeKSi_2$): C, 67.51 (67.04); H, 9.97 (9.53) %.

*Characterisation of double bond isomer Cp*Fe(η^5-Pn†H) (**5**)*

^{1}H NMR (toluene-d_8, 399.5 MHz, 303 K, selected data): δ_H 6.57 (1H, s, Pn vinylic C*H*), 3.75 (1H, d, $^3J_{HH}$ = 2.3 Hz, Pn vinylic C*H*), 3.64 (1H, d, $^3J_{HH}$ = 2.6 Hz, Pn vinylic C*H*), 2.93 (1H, dd, $^2J_{HH}$ = 22.3, $^3J_{HH}$ = 1.7 Hz, Pn allylic C*H*), 2.67 (1H, dd, $^2J_{HH}$ = 22.3, $^3J_{HH}$ = 2.5 Hz, Pn allylic C*H*), 1.76 (15H, s, Cp* C*H$_3$*), 1.31 (6H, overlapping m, ^{i}Pr C*H*), 1.21 (9H, d, $^3J_{HH}$ = 6.9 Hz, ^{i}Pr C*H*$_3$), 1.17 (18H, br, ^{i}Pr C*H*$_3$), 1.05 (6H, d, *J* = 7.1 Hz, ^{i}Pr C*H*). ^{13}C{^{1}H} NMR (C_6D_6, 125.7 MHz, 303 K, selected data): δ_C 135.85 (Pn vinylic *C*), 148.91 (Pn vinylic *C*H), 148.77 (Pn vinylic *C*-Si), 106.49 (Pn bridgehead *C*), 97.44 (Pn bridgehead *C*), 80.78 (Pn aromatic *C*), 79.30 (Cp* *C*CH$_3$), 68.52 (Pn aromatic *C*), 64.22 (Pn aromatic *C*-Si), 37.02 (Pn allylic *C*), 20.09 (^{i}Pr *C*H), 19.87 (^{i}Pr *C*H), 19.72 (^{i}Pr *C*H), 19.61 (^{i}Pr *C*H), 12.60 (^{i}Pr *C*H$_3$), 12.43 (^{i}Pr *C*H$_3$), 11.59 (Cp* C*C*H$_3$). ^{29}Si{^{1}H} NMR (C_6D_6, 79.4 MHz, 303 K, selected data): δ_{Si} 6.20, -0.66. EI-MS: *m/z* = 607 (100%), [M]$^+$. Anal. found (calcd. for $C_{36}H_{62}FeSi_2$): C, 71.13 (71.25); H, 10.20 (10.30) %.

*Synthesis of [Cp*Fe]$_2$(μ:η^5,η^5-Pn†) (**6**)*

[K]$_2$Pn† (119 mg, 0.241 mmol) in THF (15 mL) was added dropwise to a green solution of FeCp*Cl(TMEDA) (166 mg, 0.482 mmol) in THF (10 mL) at -78 °C; the reaction flask was then sealed and allowed to warm to room temperature overnight. The resulting brown suspension was stripped of solvent, and the products extracted with hot (*ca.* 80 °C) toluene (2 x 40 mL), followed by brief sonication and filtration on a frit through dry Celite. The solution was concentrated to 15 mL and the precipitated solid was warmed to *ca.* 80 °C and brought back into solution. Green crystals of **6** were formed by slowly cooling this solution to ambient temperature. A second crop of crystals was obtained by removal of the solvent from the supernatant and recrystallision of the resulting brown residues from Et_2O (3 mL) at -35 °C. Total Yield: 66 mg (34% with respect to [K]$_2$Pn†).

^{1}H NMR (toluene-d_8, 499.9 MHz, 303 K): δ_H 4.67 (2H, d, $^3J_{HH}$ = 2.1 Hz, Pn C*H*), 3.69 (2H, d, $^3J_{HH}$ = 2.1 Hz, Pn C*H*), 2.15 (6H, septet, $^3J_{HH}$ = 7.5 Hz, ^{i}Pr C*H*), 1.67 (18H, d, $^3J_{HH}$ = 7.6 Hz, ^{i}Pr C*H*$_3$), 1.54

(18H, d, $^{3}J_{HH}$ = 7.6 Hz, ^{i}Pr CH_3), 1.51 (30H, s, Cp* CH_3). $^{13}C\{^{1}H\}$ NMR (toluene-d_8, 125.7 MHz, 303 K): δ_C 102.34 (Pn bridgehead *C*), 98.50 (Pn bridgehead *C*), 87.65 (Pn *C*H), 78.06 (Cp* *C*CH_3), 65.32 (Pn *C*H), 61.20 (Pn *C*-Si), 22.10 (^{i}Pr *C*H_3), 21.65 (^{i}Pr *C*H_3), 17.20 (^{i}Pr *C*H), 11.84 (Cp* C*C*H_3). $^{29}Si\{^{1}H\}$ NMR (toluene-d_8, 79.4 MHz, 303 K): δ_{Si} 6.89. EI-MS: *m/z* = 797 (15%), $[M]^+$; 605 (100%), $[M - FeCp^*]^+$; 562 (40%), $[M - FeCp^* - {}^{i}Pr]^+$; 448 (20%), $[M - FeCp^* - Si^{i}Pr_3]^+$. Anal. found (calcd. for $C_{46}H_{76}Fe_2Si_2$): C, 69.25 (69.33); H, 9.69 (9.61) %.

Crystallographic Details

Single crystal XRD data for **2** were collected by the UK National Crystallography Service (NCS),[47] at the University of Southampton on a Bruker-Nonius FR591 rotating anode diffractometer ($\lambda_{Mo\ K\alpha}$) equipped with VariMax VHF optics and a Saturn 724+ CCD area detector. The data were collected at 120 K using an Oxford Cryosystems Cobra low temperature device. Data collected by the NCS were processed using CrystalClear-SM Expert 3.1 b18,[48] and unit cell parameters were refined against all data. Single crystal XRD data for **1**, **3**, **4**, **5** and **6**, were collected at the University of Sussex on a Bruker-Nonius Kappa CCD area detector diffractometer with a sealed-tube source ($\lambda_{Mo\ K\alpha}$), in ω scanning mode with ψ and ω scans to fill the Ewald sphere. The data were collected at 173 K using an Oxford Cryosystems low temperature device. Data were processed using Collect,[49] Scalepack, and Denzo,[50] and unit cell parameters were refined against all data. An empirical absorption correction was carried out using the Multi-Scan program.[51] Solutions and refinements were performed using WinGX[52] and software packages within. All non-hydrogen atoms were refined with anisotropic displacement parameters. All hydrogen atoms were refined using a riding model.

Computational Details

Density functional calculations were carried using the Amsterdam Density Functional package (version ADF2012.01 and ADF2014.01).[53] The Slater-type orbital (STO) basis sets were of triple-ζ quality augmented with a one polarization function (ADF basis TZP). Core electrons were frozen (C 1s; Fe 2p) in the model of the electronic configuration for each atom. The local density approximation (LDA) by Vosko, Wilk and Nusair (VWN)[54] was used together with the exchange correlation corrections of Becke and Perdew (BP86).[55,56]

ELECTRONIC SUPPLEMENTARY INFORMATION (ESI) available: Additional X-ray crystallographic and cyclic voltammetry data, schematics of DFT calculated molecular orbitals and cartesian coordinates of optimized structures are given in the ESI. CCDC 1434402–1434407 for compounds **1**–**6**. Crystallographic data available in CIF format see DOI: 10.1039/XXXXX.

AUTHOR INFORMATION

Email for FGNC: f.g.cloke@sussex.ac.uk. Email for JCG: jennifer.green@chem.ox.ac.uk.

ACKNOWLEDGEMENTS

We thank the ERC (Project 247390), the EPSRC (EP/M023885/1) and the University of Sussex for financial support. The UK National Crystallography Service (NCS) Southampton are thanked for their assistance with single crystal X-ray data collection.

REFERENCES

[1] S. Barlow, D. O'Hare, Chem. Rev. 97 (1997) 637–667.
[2] C. Lapinte, Coord. Chem. Rev. 178-180 (1998) 431–509.
[3] A. Ceccon, S. Santi, L. Orian, A. Bisello, Coord. Chem. Rev. 248 (2004) 683–724.
[4] P. Aguirre-Etcheverry, D. O'Hare, Chem. Rev. 110 (2010) 4839–4864.
[5] T.J. Peckham, P. Gbmez-Elipe, I. Manners, in:, Metallocenes, Wiley-VCH Verlag GmbH, 2008, pp. 723–772.
[6] O.T. Summerscales, F.G.N. Cloke, Coord. Chem. Rev. 250 (2006) 1122–1140.
[7] J.M. Manriquez, M.D. Ward, W.M. Reiff, J.C. Calabrese, N.L. Jones, P.J. Carroll, E.E. Bunel, J.S. Miller, J. Am. Chem. Soc. 117 (1995) 6182–6193.
[8] B. Oelckers, I. Chávez, J.M. Manriquez, E. Roman, Organometallics 12 (1993) 3396–3397.
[9] Y. Portilla, I. Chavez, V. Arancibia, B. Loeb, J.M. Manríquez, A. Roig, E. Molins, Inorg. Chem. 41 (2002) 1831–1836.
[10] E.E. Bunel, L. Valle, N.L. Jones, P.J. Carroll, C. Barra, M. Gonzalez, N. Munoz, G. Visconti, A. Aizman, J.M. Manriquez, J. Am. Chem. Soc. 110 (1988) 6596–6598.
[11] M.B. Robin, P. Day, Mixed Valence Chemistry-a Survey and Classification, Elsevier, 1968.
[12] O.T. Summerscales, S.C. Jones, F.G.N. Cloke, P.B. Hitchcock, Organometallics 28 (2009) 5896–5908.
[13] T. Tsuji, N. Hosoya, S. Fukazawa, R. Sugiyama, T. Iwasa, H. Tsunoyama, H. Hamaki, N. Tokitoh, A. Nakajima, J. Phys. Chem. C 118 (2014) 5896–5907.
[14] N. Hosoya, K. Yada, T. Masuda, E. Nakajo, S. Yabushita, A. Nakajima, J. Phys. Chem. A 118 (2014) 3051–3060.
[15] S.C. Jones, D.Phil Thesis, University of Oxford, 2003.
[16] C.J. Rivers, D.Phil Thesis, University of Sussex, 2004.

[17] T.J. Katz, M. Rosenberger, J. Am. Chem. Soc. 85 (1963) 2030–2031.
[18] D.J. Peterson, J. Org. Chem 33 (1968) 780–784.
[19] M.B. Gillies, J.E. Tønder, D. Tanner, P.-O. Norrby, J. Org. Chem 67 (2002) 7378–7388.
[20] E. Molins, W. Maniukiewicz, C. Miravitlles, M. Mas, J.M. Manríquez, I. Chavez, B. Oelckers, J. Farran, J.L. Brianso, Acta Crystallogr., Sect. C: Cryst. Struct. Commun. 52 (1996) 2414–2416.
[21] P. Seiler, J.D. Dunitz, Acta Crystallogr. Sect. B 35 (1979) 1068–1074.
[22] C. Miravitlles, E. Molins, W. Maniukiewicz, M. Mas, J.M. Manríquez, I. Chavez, B. Oelckers, A. Alvarez-Larena, J.L. Brianso, Acta Crystallogr., Sect. C: Cryst. Struct. Commun. 52 (1996) 3047–3049.
[23] A. Alvarez-Larena, J.L. Brianso, J.F. Piniella, J. Farran, J.M. Manríquez, I. Chavez, B. Oelckers, E. Molins, C. Miravitlles, Acta Crystallogr., Sect. C: Cryst. Struct. Commun. 52 (1996) 2754–2757.
[24] M.R. Churchill, K.K.G. Lin, Inorg. Chem. 12 (1973) 2274–2279.
[25] J.D. Smith, in:, Advances in Organometallic Chemistry, Elsevier, 1998, pp. 267–348.
[26] S. Jones, P. Roussel, T. Hascall, D. O'Hare, Organometallics 25 (2006) 221–229.
[27] O.T. Summerscales, D.R. Johnston, F.G.N. Cloke, P.B. Hitchcock, Organometallics 27 (2008) 5612–5618.
[28] J.C. Green, M.L.H. Green, G. Parkin, Chem. Commun. 48 (2012) 11481–11503.
[29] T.J. Katz, M. Rosenberger, R.K. O'Hara, J. Am. Chem. Soc. 86 (1964) 249–252.
[30] F.G.N. Cloke, Pure Appl. Chem. 73 (2001) 233–238.
[31] J.M. O'Connor, C.P. Casey, Chem. Rev. 87 (1987) 307–318.
[32] H.J. Gericke, N.I. Barnard, E. Erasmus, J.C. Swarts, M.J. Cook, M.A.S. Aquino, Inorg. Chim. Acta 363 (2010) 2222–2232.
[33] W.E. Geiger, F. Barrière, Acc. Chem. Res. 43 (2010) 1030–1039.
[34] R.G. Compton, C.E. Banks, Understanding Voltammetry, 2nd ed., Imperial College Press, 2011.
[35] R. Materikova, V. Babin, I. Lyatifov, T.K. Kurbanov, E. Fedin, P. Petrovskii, A. Lutsenko, J. Organomet. Chem. 142 (1977) 81–87.
[36] I. Noviandri, K.N. Brown, D.S. Fleming, P.T. Gulyas, P.A. Lay, A.F. Masters, L. Phillips, J. Phys. Chem. B 103 (2011) 6713–6722.
[37] S. Bendjaballah, S. Kahlal, K. Costuas, E. Bévillon, J.-Y. Saillard, Chem.–Eur. J. 12 (2006) 2048–2065.
[38] K.B. Wiberg, P.R. Rablen, J. Comput. Chem. 14 (1993) 1504–1518.
[39] R.S. Mulliken, J. Chem. Phys. 36 (1962) 3428–3439.
[40] F.L. Hirshfeld, Theoret. Chim. Acta 44 (1977) 129–138.
[41] C. Fonseca Guerra, J.W. Handgraaf, E.J. Baerends, F.M. Bickelhaupt, J. Comput. Chem. 25 (1993) 189–210.
[42] F.G.N. Cloke, M.C. Kuchta, R.M. Harker, P.B. Hitchcock, J.S. Parry, Organometallics 19 (2000) 5795–5798.
[43] K. Jonas, P. Klusmann, R. Goddard, Z. Naturforsch. B 50 (1995) 394–404.
[44] M. Schlosser, J.R. Hartmann, Angew. Chem. Int. Ed. Engl. 12 (1973) 508–509.
[45] R.B. King, M.B. Bisnette, J. Organomet. Chem. 8 (1967) 287–297.
[46] P. Kovacic, N.O. Brace, J. Am. Chem. Soc. 76 (1954) 5491–5494.
[47] S.J. Coles, P.A. Gale, Chem. Sci. 3 (2012) 683–689.
[48] Rigaku, CrystalClear (2011).
[49] Bruker-AXS BV, Collect (1997).
[50] Z. Otwinowski, W. Minor, Methods Enzymol. 276 (1997) 307.

[51] R.H. Blessing, Acta Crystallogr., A, Found. Crystallogr. 51 (1995) 33–38.
[52] L.J. Farrugia, J. Appl. Crystallogr. 32 (1999) 837–838.
[53] SCM, Amsterdam Density Functional, ADF (2006).
[54] S.H. Vosko, L. Wilk, M. Nusair, Can. J. Phys. 58 (1980) 1200–1211.
[55] A. Becke, Phys. Rev., A 38 (1988) 3098–3100.
[56] J.P. Perdew, Phys. Rev. B 33 (1986) 8822–8824.